Research Square

Preprints are preliminary reports that have not undergone peer review.
They should not be considered conclusive, used to inform clinical practice,
or referenced by the media as validated information.

Comprehensive comparison of promoters from the Ethanol Utilization Pathway of Komagataella phaffii

Dominic Goj
Austrian Centre of Industrial Biotechnology (Austria)
Karin Reicher
Austrian Centre of Industrial Biotechnology (Austria)
Azra Bjelic
Graz University of Technology, NAWI Graz
Claudia Rinnofner
claudia.rinnofner@mybios.at

myBIOS GmbH
Margit Winkler
ZHAW Zurich University of Applied Sciences

Research Article

Keywords: Komagataella phaffii, ethanol utilization pathway (EUT), promoter studies, ADH2 / ADH900, yeast engineering, protein expression

Posted Date: September 25th, 2026

DOI: https://doi.org/10.21203/rs.3.rs-10991501/v1

License: This work is licensed under a Creative Commons Attribution 4.0 International License.
Read Full License

Additional Declarations: No competing interests reported.

Comprehensive comparison of promoters from the Ethanol Utilization Pathway of *Komagataella phaffii*

Dominic Goj[1,2], Karin Reicher[1], Azra Bjelic[2], Claudia Rinnofner[4] and Margit Winkler[1,3*]

[1]Austrian Centre of Industrial Biotechnology, Petersgasse 14, Graz, Austria.

[2]Institute of Molecular Biotechnology, Graz University of Technology, NAWI Graz, Petersgasse 14, Graz, Austria.

[3]ZHAW Institute of Chemistry and Biotechnology, Einsiedlerstrasse 31, 8820 Wädenswil, Switzerland.

[4]myBIOS GmbH, ZWT, Neue Stiftingtalstraße 2, Graz, Austria

[*]Corresponding author at: ZHAW Institute of Chemistry and Biotechnology, Einsiedlerstrasse 31, 8820 Wädenswil, Switzerland.

E-mail addresses: margit.winkler@zhaw.ch

Abstract

Background

Ethanol (EtOH) represents a promising carbon source for microbial fermentations, aimed at sustainable production of recombinant proteins for food and agricultural applications. However, EtOH-regulated expression systems in *Komagataella phaffii* remain poorly characterized. To address this gap, we investigated the regulation of promoters within the EtOH utilization (EUT)

pathway i.e. *alcohol dehydrogenase 2* and 900 (P_{ADH2}/P_{ADH900}), *aldehyde dehydrogenase 4* (P_{ALD4}) and *acetyl-CoA synthetase 1* and *2* (P_{ACS1}/P_{ACS2}).

Results

We analyzed the activities of EUT promoters in wild-type and knock strains lacking *ADH2* and *ADH900* across different carbon sources, measuring reporter protein levels and resulting extracellular metabolite profiles. Δ*adh2* and Δ*adh2*+Δ*adh900* strains showed impaired growth on EtOH, while Δ*adh900* displayed slightly reduced growth. The wild-type produced 2.0 ± 0.9 g L^{-1} EtOH on 1% glucose and Δ*adh900* strain still produced up to 1.5 ± 0.5 g L^{-1}. EtOH feeding experiments showed that 1% EtOH in minimal medium optimally supported eGFP expression, whereas higher concentrations (up to 12%) limited both growth and expression. Independent of carbon source, P_{ADH2}-driven eGFP expression was similar in the wild-type, yet eGFP produced per cell increased in knockout strains. P_{ALD4} was upregulated in Δ*adh2* mutants during growth on glucose while $P_{ACS1/2}$ and P_{ALD4} were upregulated in Δ*adh900* strains grown on EtOH. P_{ADH900} was repressed and P_{ACS1} promoter was upregulated by EtOH.

Conclusion

ADH2 is primarily responsible for EtOH consumption, while ADH900 contributes to EtOH production, though single knockouts revealed a functional overlap: Δ*adh900* still produced EtOH, and Δ*adh2* displayed minimal growth on EtOH. In both single knockouts, residual EtOH levels remained on glucose. Our findings give new insights on the regulation of EUT promoters and their role in *K. phaffii*'s EtOH metabolism: Δ*adh2* and Δ*adh900* cells rendered P_{ADH2}-driven expression to be more EtOH-responsive than in the wild-type due to impaired EtOH consumption leading to more stable EtOH levels. P_{ALD4} likely responds to accumulating EtOH in Δ*adh2* on glucose while

$P_{ACS1/2}$ and P_{ALD4} are upregulated in Δ*adh900* on EtOH, assumingly due to elevated acetaldehyde or acetate levels with blocked reduction of acetaldehyde to EtOH.

Keywords: *Komagataella phaffii*, ethanol utilization pathway (EUT), promoter studies, ADH2 / ADH900, yeast engineering, protein expression

1. Background

Komagataella phaffii is a methylotrophic, Crabtree-negative yeast that has become a widely used host for recombinant protein expression. Primary advantages of using *K. phaffii* as an expression host include its ability to grow quickly to high cell densities under respiratory conditions, its efficient secretory pathway, and its ability to perform diverse posttranslational modifications of proteins (Cereghino and Cregg, 1999; Higgins and Cregg, 1998; Li *et al*., 2007). The Methanol Utilization Pathway (MUT) of *K. phaffii* is a key metabolic route that enables the utilization of methanol as a carbon source for growth (Fig. 1). AOX1/2 convert methanol into formaldehyde which can then take two different routes – the assimilative or the dissimilative branch. In the assimilative pathway, formaldehyde is sequentially converted to dihydroxyacetone phosphate and supplied to the pentose phosphate pathway (PPP) to be converted to biomass. In the dissimilative pathway, formaldehyde is ultimately converted to CO_2 by formaldehyde dehydrogenase (FLD), S-formylglutathione hydrolase (FGH) and formate dehydrogenase (FDH), while producing NADH (Berrios *et al*., 2022). The *AOX1* promoter (P_{AOX1}) in Mut^S (Δ*aox1*) strains is widely used for high-level expression of proteins and is tightly regulated and strongly induced by methanol (Krainer *et al.*, 2012) accompanied by extensive peroxisomal proliferation (Van Der Klei *et al*., 2006) and slow cell growth. However, the short chain alcohol methanol - flammable and toxic - raises concerns, particularly when handled in large volumes during industrial-scale fermentations. Consequently, alternative inducible expression systems that do not rely on methanol as an inducer

have been developed, for instance, a monosodium glutamate-inducible expression system in *K. phaffii* (Rajak *et al*., 2024). Synthetic circuits have also been established to allow for alcohol-responsive expression. Wang *et al.* used the ethanol-induced transcriptional signal amplification device (ESA), originally published by Liu *et al.* (2019), to control the expression of α-human lactalbumin, where ethanol indirectly promoters transcription from the *AOX1* core promoter, uncoupled from methanol induction (Wang *et al.,* 2025). Mattanovich *et al.* demonstrated glucose-regulated recombinant protein expression in *K. phaffii* using the high-affinity glucose transporter promoter P_{GTH1}, which outperformed a classical methanol fed-batch strategy (Prielhofer *et al*., 2018). EtOH is less toxic and poses fewer concerns for food applications and operational safety, and yeasts are able to utilize EtOH as a carbon source. Especially renewable bioethanol, a side-stream product of multiple industrial processes, could be used as a carbon source for microbes to produce proteins for the agricultural and food sector (Van Peteghem *et al*., 2022). Various EtOH-regulated or EtOH-inducible expression systems have been studied, such as the EtOH-inducible *alcohol dehydrogenase 2* (P_{ADH2}) promoter of *K. phaffii* (Cregg and Tolstorukov, 2012). *ADH2* (*PAS_chr2-1_0472,* formerly *ADH3)* was reported to be the sole gene responsible for EtOH utilization, as Δ*adh2* mutants were unable to consume EtOH (Karaoglan *et al*., 2016). Another key enzyme in *K. phaffii*'s EtOH metabolism is ADH900 (*PP7435_Chr2-0990*), which plays a central role in EtOH production [(Karaoğlan et al., 2020), (Figure 1)]. Although *K. phaffii* is classified as a Crabtree-negative yeast, glucose overflow metabolism and oxygen depletion results in EtOH formation at concentrations ranging from 1 to 2% (Baumann *et al*., 2010; Karaoğlan *et al*., 2020; Steimann *et al*., 2024*)*. Transcriptional control of the EUT pathway in *K. phaffii* is exerted by two *S. cerevisiae* transcription factor homologues, Cat8-1 and Cat8-2, which are required for growth on C2 carbon sources. Barbay *et al.* (2021) showed that the two factors jointly activate *ADH2*, *ALD4* and *ACS1*, whereas gluconeogenic genes, such as *FBP1* and *PCK1*, are regulated

91 independently of them. *CAT8-1* transcript levels were two- to fourfold higher on ethanol and
92 methanol than on glucose or glycerol. The carbon source responsive element (CSRE) motif,
93 recognized by Cat8 in *S. cerevisiae*, was predicted in the promoter regions of all three target genes.
94 The genes of ethanol assimilation are therefore not controlled independently, but share a common
95 transcriptional factor, which is upregulated by the presence of C1 and C2 alcohols. Çalık *et al.*
96 engineered the *ADH2* promoter to enhance recombinant protein expression on EtOH by replacing
97 specific transcription factor binding sites with synthetic motifs for binding of Mxr1, Cat8 and Aca1
98 transcription factors. The introduction of a Cat8 binding site proved to be effective as this
99 modification resulted in 3.7-fold higher GFP titers on minimal medium containing 2% EtOH
100 compared to the wild-type *ADH2* promoter (Ergün *et al*., 2019).

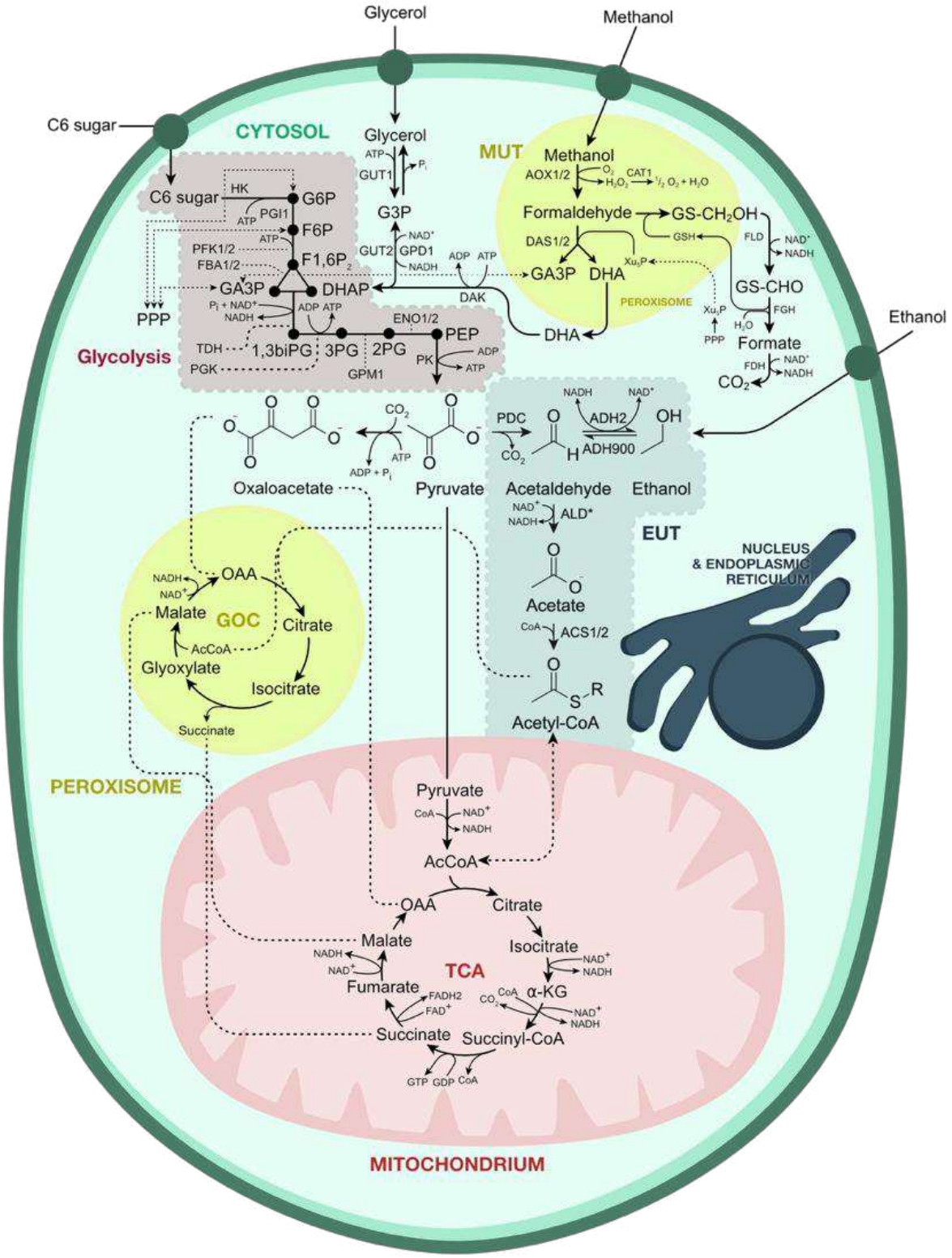


Fig. 1: Overview of key pathways involved in the degradation of C6-sugars, glycerol, methanol and ethanol in *K. phaffii*. Enzymes: ACS1/2 = acetyl-CoA synthetase (Nocon *et al.*, 2014), ADH2/900 = alcohol dehydrogenase

(Karaoğlan *et al*., 2020), ALD = aldehyde dehydrogenase (Nocon *et al*., 2014), AOX1/2 = alcohol oxidase, CAT1 = catalase 1, DAK = dihydroxyacetone kinase, DAS1/2 = dihydroxyacetone synthase (Berrios *et al*., 2022; Hartner and Glieder, 2006), FBA1/2 = fructose-1,6-bisphosphate aldolase, FDH = formate dehydrogenase, FGH = S-formylglutathione hydrolase, FLD = S-(hydroxymethyl)glutathione dehydrogenase (Berrios *et al*., 2022; Hartner and Glieder, 2006), GPM1 = phosphoglycerate mutase, GUT1/2 = glycerol kinase, HK = hexokinase, PDC = pyruvate decarboxylase, PFK1/2 = phosphofructokinase, PGI1 = glucose-6-phosphate isomerase, PK = pyruvate kinase, TDH = glyceraldehyde-3-phosphate dehydrogenase. Compounds: 1,3biPG = 1,3-biphospho-glycerate 2PG = 2-phospho-glycerate, 3/2PG = 3/2-phospho-glycerate, DHA(P) = dihydroxyacetone (phosphate), $F1,6P_2$ = fructose-1,6-bisphosphate, F6P = fructose-6-phosphate, G3P = *syn*-glycerol-3-phosphate, G6P = glucose-6-phosphate, GA3P = glyceraldehyde-3-phosphate, GS-CH_2OH = S-(hydroxymethyl)glutathione, GS-CHO = S-formylglutathione, PEP = phosphoenolpyruvate. Pathways: EUT = Ethanol Utilization Pathway, MUT = Methanol Utilization Pathway, PPP = Pentose Phosphate Pathway. Enzymes and pathways were sourced from Flores (2000) and YeastPathways (https://pathway.yeastgenome.org) as well as KEGG Database (https://www.kegg.jp).

Recently, transcriptome-guided screening, based on expression strength, has been applied to identify ethanol-responsive promoters in *K. phaffii* (Liu *et al.*, 2025). The authors recovered 36 endogenous ethanol-indubile promoters from a glucose-ethanol transcriptome comparison and combined the most active upstream regulatory sequences with strong core promoters, yielding synthetic promoters that outperformed P_{AOX1} by up to 4.5-fold. However, a systematic, side-by-side characterization of the native EUT pathway promoters across multiple carbon sources, and in diverse genetic backgrounds, unable to consume or produce EtOH, has not been reported yet, to our knowledge, with a reporter protein-based screening method. Therefore, we aimed at a comprehensive evaluation to close this gap. To prevent EtOH to be overly consumed and channeled into growth, the key gene for EtOH consumption was knocked out to create a phenotype which is unable to grow on EtOH as a sole carbon source. Further, to suppress EtOH formation under fermentative conditions by ADH900 mediated acetaldehyde reduction, we created *ADH900*

knockout strains to determine protein expression and EtOH levels on glucose and other carbon sources.

2. Methods

Chemicals, media and media ingredients were purchased from Carl Roth GmbH, VWR International LLC or ThermoFisher Scientific Inc. unless stated otherwise. Materials for cloning and purification of DNA were purchased from New England Biolabs. These included Q5 HF DNA Polymerase, Q5 Reaction Buffer, Monarch Plasmid Miniprep Kit and Gel Extraction Kit. Fast digest enzymes and buffers were ordered from ThermoFisher Scientific Inc.

2.1 Strains, plasmids and DNA sequences

E. coli Top10 was used as a cloning host. *K. phaffii* CBS2612 was used to generate knockout and reporter strains. A full list of all reporter plasmids can be found in the supplementary information (Table S2) which include multiple combinations of up to eight different promoters upstream to the reporter gene sequence of *eGFP*. The selected promoters were P_{AOX1}, P_{DAS1}, P_{DAS2}, P_{ADH2}, P_{ALD4}, P_{ACS1}, P_{ACS2}, and P_{ADH900}. The promoter sequences were either amplified from synthetic fragments (IDT, Twist Bioscience) or from *K. phaffii* CBS2612 genomic DNA. A complete list of all used promoter sequences can be found in the supplementary information (Table S1).

2.2 Cloning of reporter plasmids

All reporter-constructs were assembled with Gibson Assembly. Fragments for the assembly were vector backbones (amplified from existing vectors), promoter sequences (synthetic fragments or amplified from *K. phaffii* genomic DNA) and *eGFP* (synthetic gene). Electrocompetent *E. coli* Top10 cells were transformed with assembled plasmids. Plasmids were sequenced and confirmed before linearization and transformation of electrocompetent *K. phaffii* cells. To clone eGFP reporter constructs, the backbone of the pPpT5 vector (vector V1, Fig. S3) was amplified. The fragment

contained 5' and 3' *eGFP* sequence overhangs for the assembly with the *eGFP* fragment (S2.3). The resulting vector V3 was used as a template for the cloning of the other eGFP reporter constructs containing promoter sequences from Table S1.

2.3 Generation of Komagataella phaffii knockout strains

Targeted gene replacements were performed according to the methods described by Näätsaari *et al.* (2012). Knockout strains, *K. phaffii* CBS2612 Δ*ADH2* (P5), *K. phaffii* CBS2612 Δ*ADH900* (P107) and *K. phaffii* CBS2612 Δ*ADH2* Δ*ADH900* (P109) were generated from wild-type *K. phaffii* CBS2612 (P0). For each knockout, 500 ng of two overlapping fragments - representing the knockout cassette - were integrated. A detailed description of knockout-cloning can be found in the supporting materials (S1.1).

Transformed cells were streaked on YPD-Zeocin plates (100 µg mL^{-1} Zeo) and incubated at 28 °C for two days. Transformants were picked and streaked (1) on YPD-Zeo plates for genomic DNA isolation and subsequent confirmation of gene knock-out at the target locus by colony PCR or genome sequencing and (2) on minimal media agar plates with 0.5% methanol (MM) for marker curing. Two rounds of marker curing were performed by re-streaking picked colonies from MM plates on fresh MM plates.

2.4 Generation of Komagataella phaffii reporter strains

Reporter plasmids were linearized with BglII Fast Digest and purified from a preparative DNA agarose gel, except for P_{ADH2} containing plasmids, which were linearized with *Kpn*I. Electrocompetent P0, P5, P107 and P109 cells, prepared according to Lin-Cereghino *et al.* (2005), were transformed with 500 ng of each linearized construct.

2.5 General cultivation conditions

In general, plates and liquid overnight cultures contained 100 µg mL^{-1} Zeocin. LB-Zeo plates were used for plating *E. coli* transformants and YPD-Zeo plates for plating *K. phaffii* transformants. *E.*

176 *coli* cell cultures were incubated at 37 °C for 16 hours shaking at 120 rpm. For *K. phaffii*, pre-
177 cultivations were performed at 28 °C and 130 rpm for 16 hours. Usually, liquid cultures of single,
178 isolated clones did not contain antibiotics. Liquid shake flask pre-cultures and main-cultures of *K.*
179 *phaffii* were grown in 100 or 300 mL baffled shake flasks filled with 25 or 50 mL 1% BMD or 1%
180 BMG cultivation medium, respectively. Liquid 96 deep well plate pre-cultures and main-cultures
181 of *K. phaffii* were grown in 250 µL 1% BMD cultivation medium. *K. phaffii* main-cultures in 96
182 deep well plates (DWP) were inoculated with 10% inoculum from the pre-culture, whereas shake
183 flask main-cultures were inoculated to an optical cell density (OD_{600}) of 0.1. Main cultures were
184 cultivated for 3 days before the feeding phase started. The general feeding phase had a duration of
185 two days and consisted of two feed pulses per day (6 to 8 hours time-difference) with the aim to
186 achieve 1% levels of the target carbon source (BMX) in the medium. Three different carbon sources
187 were used as feed: (1) Glucose (D), (2) Glycerol (G), and (3) Ethanol (E). Feed media for 96-DWP
188 cultivations always consisted of 1x YNB, 100 mM potassium phosphate buffer (pH 6), double
189 distilled water and 0.4 mg L^{-1} biotin. Feed media for 96-DWP cultivations contained 2% or 10%
190 of the target carbon source. 96-DWP cultures were fed according to the following scheme: (1) 250
191 µL of 2% BMX, and (2) 3x 50 µL 10% BMX, respectively. Feeding of shake flask cultures was
192 performed accordingly with the same relative volumes.

193 *2.6 Growth experiment with K. phaffii strains in different media*

194 To test growth behavior of *K. phaffii* strains on different carbon sources, pre-cultures were prepared
195 in 100 mL baffled shake flasks with 25 mL BMD1 and shaken for 72 h at 28 °C and 130 rpm. Main
196 cultures were inoculated with 0.1 OD_{600} units in 300 mL baffled shake flasks with BMD1, BMG1
197 or BME1 in triplicates and cultivated for at least 48 hours at 28 °C and 130 rpm. Cultures were fed
198 at the following time points with 5 mL of BMX10: 6 hours, 24 hours and 30 hours after main

199 culture inoculation. Optical densities were measured at 600 nm. Samples of 1 mL were withdrawn
200 for HPLC analysis immediately before the feeding pulse.

201 *2.7 HPLC analysis of media and cultures*

202 Samples (1 mL) were centrifuged for 15 minutes at 15,000 rcf. 200 µL of culture supernatant was
203 transferred to HPLC glass vials with inserts. For analysis, a Shimadzu HPLC system was used with
204 a Biorad Aminex HPX-87H column. Analytes were eluted in a 30 min isocratic method with 5 mM
205 H_2SO_4 dissolved in ultrapure, filtered water at a flow rate of 0.6 ml/min and a column oven
206 temperature of 65°C. To detect and quantify glucose, glycerol, acetate and EtOH, an RI detector
207 (RID-20A, Shimadzu) was used whereas acetaldehyde was detected via UV at 254 nm (SPD-M40,
208 Shimadzu). Calibration curves were established with the following concentrations: for glucose,
209 glycerol, EtOH: 45, 36, 29.25, 22.5, 18, 13.5, 9, 6.75, 4.5, 2.25, 1.35 and 0.45 g L^{-1}, for acetate: 6,
210 4.8, 3.9, 3, 2.4, 1.8, 1.2, 0.9, 0.6, 0.3, 0.18 and 0.06 g L^{-1} and for acetaldehyde: 1, 0.8, 0.65, 0.5,
211 0.4, 0.3, 0.2, 0.15, 0.1, 0.05, 0.03 and 0.01 g L^{-1}, respectively.

212 *2.8 Screening of promoter activity in reporter strains*

213 The effects of different promoter and knock-out combinations on the expression of eGFP and
214 growth of the reporter strains were assessed by fluorescence and absorbance measurements. 36 to
215 72 transformants per strain-reporter combination were screened. Clones were picked with sterile
216 toothpicks from transformation plates to inoculate 250 µL of 1% BMD (BMD1) in DWPs.
217 Negative controls were P0, P5, P107 or P109 – not carrying the reporter construct – and were
218 cultivated and measured in 8 replicates on each plate. 8 sterile controls were included as well on
219 every plate. As a positive control, a singularized *K. phaffii* CBS 2612 P_{ADH2}:*eGFP* clone (P31) was
220 implemented at a later stage and cultivated in octuplicates.

2.8.1 Screening of eGFP and optical densities in 96-deep well plates

10 µL or 20 µL of culture was mixed with 190 µL or 180 µL of double distilled water, respectively, in flat-bottom black 96 well microtiter plates (MTP). A SynergyMX plate-reader from BioTek was used to measure fluorescence of eGFP with an excitation and emission wavelength of 488 nm and 507 nm, respectively. Optical cell density was measured at 600 nm. Values recorded were used to calculate a median value of (1) eGFP fluorescence, (2) optical density and (3) eGFP fluorescence normalized to the optical density for clones belonging to the same promoter-reporter-strain group. OD_{600} normalized eGFP values were calculated per clone by dividing its eGFP readout by its OD_{600} readout. eGFP readouts below 500 and OD_{600} readouts below 0.08 were cut-off as these values were not significantly different to the negative controls.

2.8.2 Effect of EtOH concentration on eGFP expression under the control of P_{ADH2} and P_{ALD4}

8 randomly picked clones of reporter strains P0 (*K. phaffii* wild-type) and P5 (*K. phaffii* Δ*adh2*) transformed with P_{ADH2}:*eGFP* and P_{ALD4}:*eGFP*, respectively, were pre-cultured as described above in 96-DWPs. Main cultures were inoculated in 250 µL BMD1 and cultivated for three days at 28 °C, 320 rpm. Main cultures were fed two times on day four and two times on day five with 100 µL of minimal media containing 1.5%, 3%, 6%, 12% or 18% EtOH. eGFP and OD_{600} measurements were carried out on day six, as described in section 2.8.1.

3. Results

3.1 Growth of knockout strains on different carbon sources

Three different genetically modified strains, P5 (Δ*adh2*), P107 (Δ*adh900*) and P109 (Δ*adh2* Δ*adh900*) were derived from the *K. phaffii* CBS 2612 wild-type P0 strain. As shown in Fig. 2, all strains followed a similar growth behavior when grown in BMD1 and BMG1 for two to three days in shake flasks and could achieve optical densities of up to 15 ± 1.2 units.

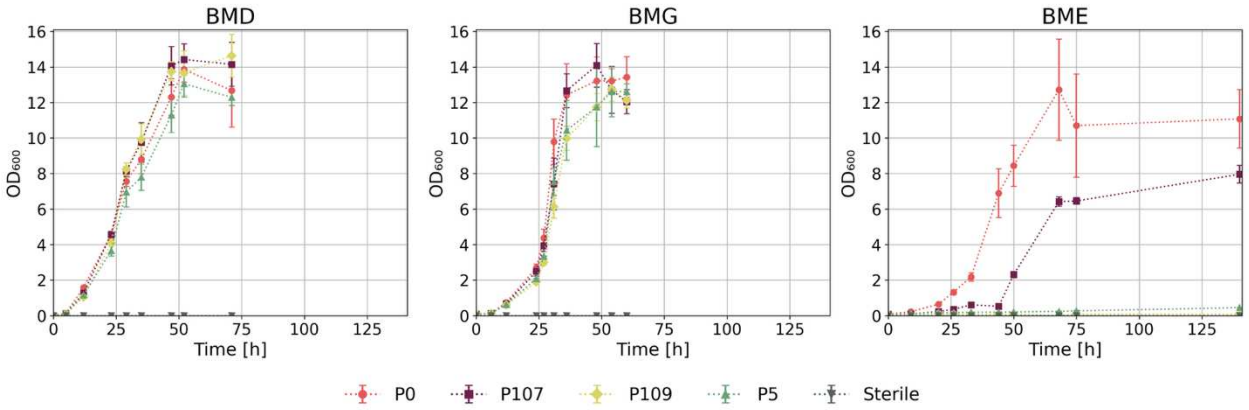


Fig. 2: Growth profile (mean optical densities measured at 600 nm) of strains P0 (*K. phaffii* CBS 2612), P5 (*K. phaffii* CBS2612 Δ*ADH2*), P107 (*K. phaffii* CBS2612 Δ*ADH900*) and P109 (*K. phaffii* CBS2612 Δ*ADH2* Δ*ADH900*) on different carbon sources in shake flasks. Cultures (50 mL) were inoculated to an OD_{600} of 0.1 in minimal medium with 1 wt% of the carbon sources: glucose (BMD1), glycerol (BMG1) or EtOH (BME1). Each combination was cultivated in triplicates. Feeding was pursued at regular timepoints with 5 mL of BMX10.

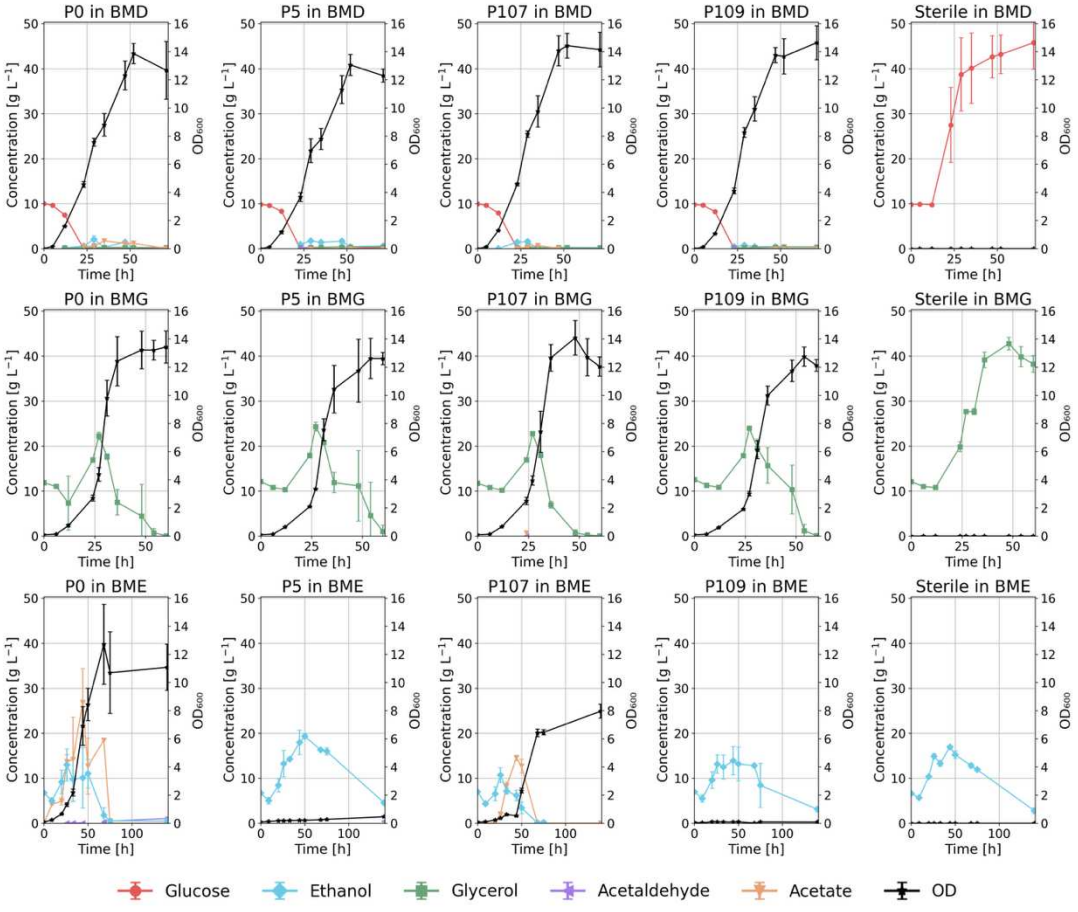


Fig. 3: Mean analyte concentrations [g L^{-1}] quantified in cultivation media BMD1, BMG1 and BME1 inoculated with strains P0, P5, P107 and P109 and cultivated in shake flasks (triplicates). Mean optical densities were measured at 600 nm (right axis).

In the presence of EtOH as the sole carbon source, wild-type *K. phaffii* (P0) achieved 11.1 ± 1.6 OD_{600} units after a prolonged lag-phase (t=140 h). As expected, P5 and P109 exhibited impaired growth on EtOH as the sole carbon source. P5 reached an OD of 0.45 ± 0.01 after 140 hours of cultivation while P109 OD values remained at 0.1. The concentration of the carbon sources supplied and consumed as well as excreted fermentation products such as EtOH, acetate and acetaldehyde are shown in Fig. 3. Samples were withdrawn from the cultivation media at regular timepoints before each feeding pulse and analyzed by HPLC. Interestingly, when *K. phaffii* was grown in BMD1, EtOH could be detected in all samples (Fig. 3 top). P107 and P109, assumed to produce no EtOH at all, showed EtOH concentrations of up to 1.53 ± 0.52 g L^{-1} (t=29 h) and 0.44 ± 0.03 g L^{-1} (t=23 h), respectively. P5 accumulated up to 1.70 ± 0.20 g L^{-1} of EtOH (t=29 h) and P0 up to 2.02 ± 0.86 g L^{-1} of EtOH (t=29 h). Acetate was found in only one sample of P0 (1.71 g L^{-1}) and one sample of P107 (0.66 g L^{-1}) in BMD1, while acetaldehyde was detected only in P5 (0.12 ± 0.02 g L^{-1}) and P109 (0.092 ± 0.007 g L^{-1}).

When grown in BME, P0 and P107 fully metabolized the EtOH after 69 and 75 hours of cultivation, respectively, and up to 26.8 ± 7.3 g L^{-1} and 14.5 ± 0.6 g L^{-1} of acetate was detected (Fig. 3, bottom). By contrast, no EtOH was consumed by P5 and P109 and no acetate was formed. In P0 and P107, EtOH was converted to acetaldehyde by ADH2, likely followed by an oxidation reaction to acetate *via* aldehyde dehydrogenase and subsequent conversion to acetyl-CoA by acetyl-CoA synthetases. In P5 and P109 samples, EtOH concentrations declined over time and 4.5 ± 0.1 g L^{-1} and 3.0 ± 0.6 g L^{-1} were detected at the end of the cultivation (140 h), respectively. EtOH concentrations also

declined in a similar manner in the sterile control. The glycerol concentration profile of P0, P5, P107 and P109 looked similar for all the strains (Fig. 3, middle).

3.2 Effect of EtOH concentration on eGFP expression under control of P_{ADH2} and P_{ALD4}

Octuplicates of strains P0 and P5 were cultivated in 96-DWPs with varying EtOH concentrations (0.5% to 12%) to identify the optimal conditions for growth and eGFP expression. As summarized in Table 1, the highest biomass formation was observed at an EtOH concentration of 1% in both strains. At lower concentrations (0.5%), P0 gave significantly less cell density (~30%), while the effect on P5 was minor (~8%). At higher concentrations, growth of P0 was impaired, whereas P5 remained largely unaffected.

Table 1: Mean maximal optical cell densities (OD_{600}) by strains P0 and P5 (P_{ADH2}:eGFP and P_{ALD4}:eGFP) in 96-deep well plates fed with different EtOH concentrations. EtOH concentration in percentages refers to the targeted final concentration of EtOH in each well. 8 clones per strain and reporter construct were cultivated.

	OD_{600}	
EtOH [%]	**P0**	**P5**
0.5%	10.1 ± 1.0	4.7 ± 1.2
1%	14.4 ± 2.6	5.1 ± 1.4
2%	11.5 ± 1.3	4.6 ± 1.0
4%	4.5 ± 0.9	3.8 ± 0.4
8%	3.6 ± 0.7	2.8 ± 0.3
12%	4.3 ± 1.1	3.1 ± 0.6

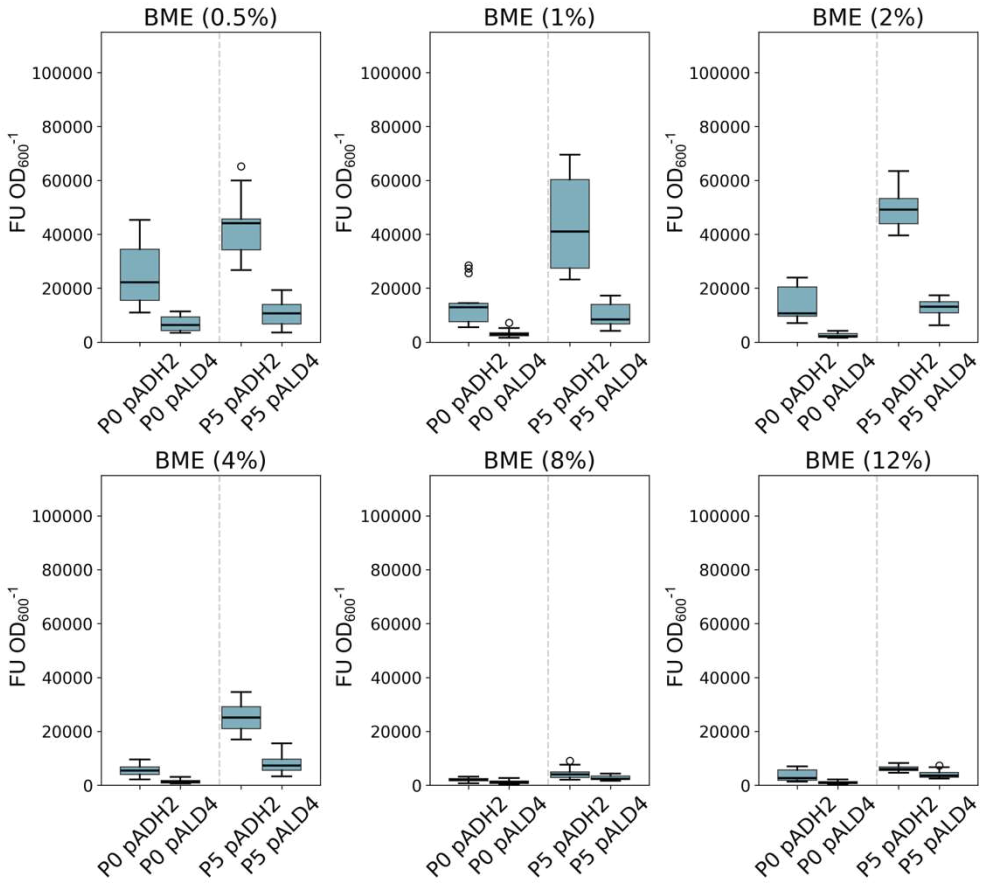


Fig. 4: Fluorescence units relative to optical densities [FU OD_{600}^{-1}] for reporter strains P0 and P5 expressing eGFP under P_{ADH2} and P_{ALD4}, respectively. 8 clones per strain and reporter construct were cultivated.

Fig. 4 presents the fluorescence normalized to cell density in strains P0 and P5 expressing eGFP under the control of P_{ADH2} and P_{ALD4}. Absolute fluorescence of the strains and optical densities are shown in Fig. S4 and S5. For P_{ADH2} in P0, absolute median fluorescence values were highest [204,000 fluorescent units (FU)] at 0.5% EtOH and decreased with increasing EtOH input to 133,00 FU at 2% EtOH. 4% EtOH resulted in a pronounced drop (23,000 FU) and minimal eGFP production at higher EtOH concentrations. A comparable trend was observed for P_{ALD4}. Importantly, this decline in fluorescence was not solely attributable to reduced biomass, as normalized median values also decreased markedly from 22,000 FU OD_{600}^{-1} to 2,100 FU OD_{600}^{-1} for P_{ADH2} in P0 and from 6,300 FU OD_{600}^{-1} to 1,000 FU OD_{600}^{-1} for P_{ALD4} in P0 between 0.5% and 12% EtOH. Similarly, fluorescence values decreased in P5 with increasing EtOH concentrations.

3.3 eGFP expression by knockout strains under the control of different promoters and grown on different carbon sources

The wild-type *K. phaffii* and the knock-out strains P5, P107 and P109 were transformed with 8 different reporter constructs, each containing the *eGFP* gene under the control of a variety of promoters. 36 to 72 clones were picked per combination and cultivated in 96-DWPs. To compensate the effect of potential multicopy and different loci integrations, a landscape of clones was screened, and the data is presented as boxplots. The cultivation followed a classical strategy which was comprised of a (1) batch phase on BMD1 for 3 days and (2) a phase of pulse-feeding four different carbon sources over two days. Then, the cultures were screened for fluorescence to assess the amount of eGFP in fluorescence units (FU) - influenced by the choice of promoter and genetic modification. Collected results of the cultures' eGFP levels and OD_{600} are shown in Fig. 5, Fig. 6 and Fig. 7. Fig. 8 shows a subset of strains where eGFP was expressed under only EUT pathway promoters. Fig. S4 and S5 show the normalized eGFP levels as well as OD_{600} units achieved.

3.3.1 Growth of strains on different carbon sources in 96-deep well plates

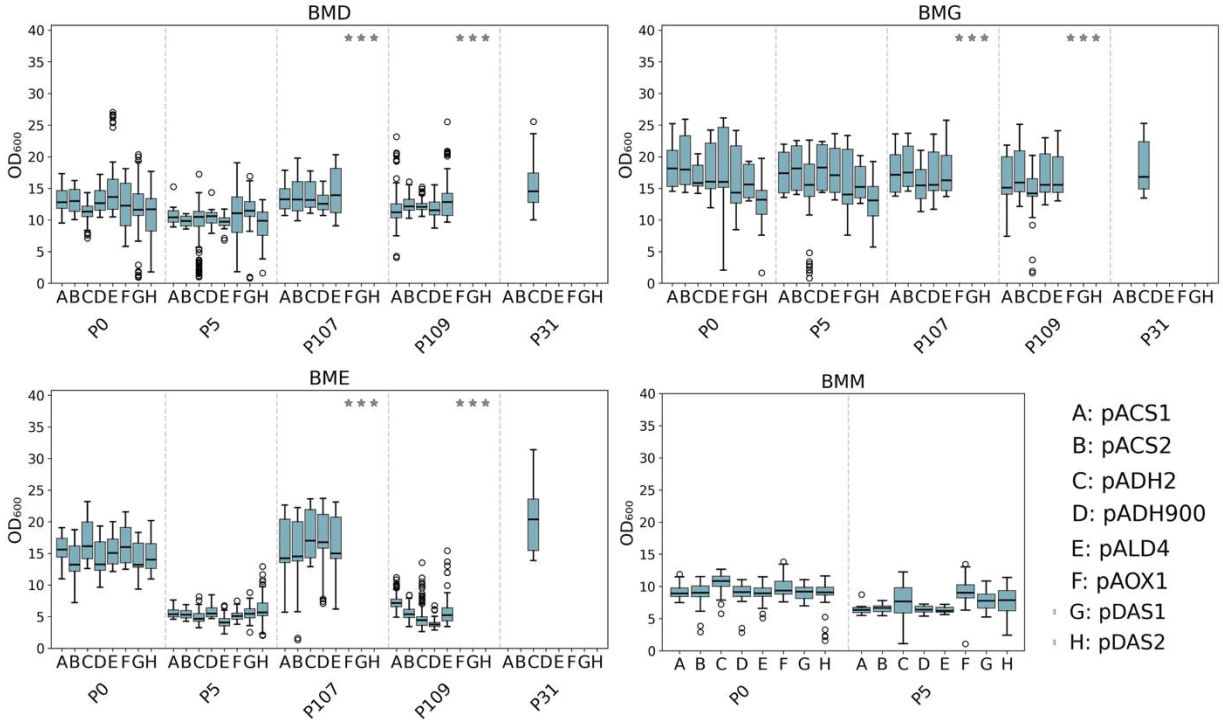


Fig. 5: Cell density of cultures [OD_{600}] at the end of the cultivation. 36 to 72 clones of each reporter construct were cultivated in 96-deep well plates. Each cultivation plate was spiked four times over two days with one of the four minimal media variants (BMD1, BMG1, BME1 and BMM1). Control strains P0, P5, P107 and P109 lacking the reporter construct and sterile controls were cultivated in octuplicates (data not shown). P31 = singularized clone of *K. phaffii* CBS 2612 P_{ADH2}:eGFP (Positive control) cultivated in octuplicates. Star = strains not created.

K. phaffii CBS2612 wild-type strain (P0) achieved OD_{600} units in the range of 12 (on BMD1) to almost 20 (BMG1) with the lowest median optical densities reached on BMM1 (Fig. 5). *K. phaffii* CBS2612 Δ*ADH2* (P5) and *K. phaffii* CBS2612 Δ*ADH2* Δ*ADH900* were expected to show impaired growth on EtOH which was confirmed in the previous chapter. Growth of cells was only observed during the cultivation phase on BMD1, before feeding with EtOH started (~ 5 OD_{600} units). Among all conditions, glycerol appeared to be the most favorable carbon source in terms of optical density achieved (15 to 20 OD_{600} units, Fig. 5). Biomass yields on BMD and BME were similar (10-15 OD_{600} units, Fig. 5) for P0 and P107 while P5 and P109 were strongly growth-

inhibited (4-7 OD_{600} units). Methanol, in the applied concentration, appeared to be growth-inhibiting as only 5 to 10 OD_{600} units were achieved during the cultivation for all reporter strains.

3.3.2 eGFP expression in strains cultivated on different carbon sources

Methanol inducible promoters, such as P_{AOX1} and $P_{DAS1/2}$, which were originally included as a benchmark, yielded the highest total eGFP readouts on BMM (Fig 6. BMM) and were strongly repressed on alternative carbon sources. Total eGFP expression in P0 under P_{AOX1} control was 30-fold lower on BMD, 27-fold lower on BME and 22-fold lower on BMG compared to BMM (median total eGFP readouts). In P5 P_{AOX1}, total eGFP was 1.4-fold lower compared to P0 P_{AOX1}, with repression being particularly pronounced on BME. P_{DAS1} and P_{DAS2} consistently showed lower eGFP levels than P_{AOX1}.

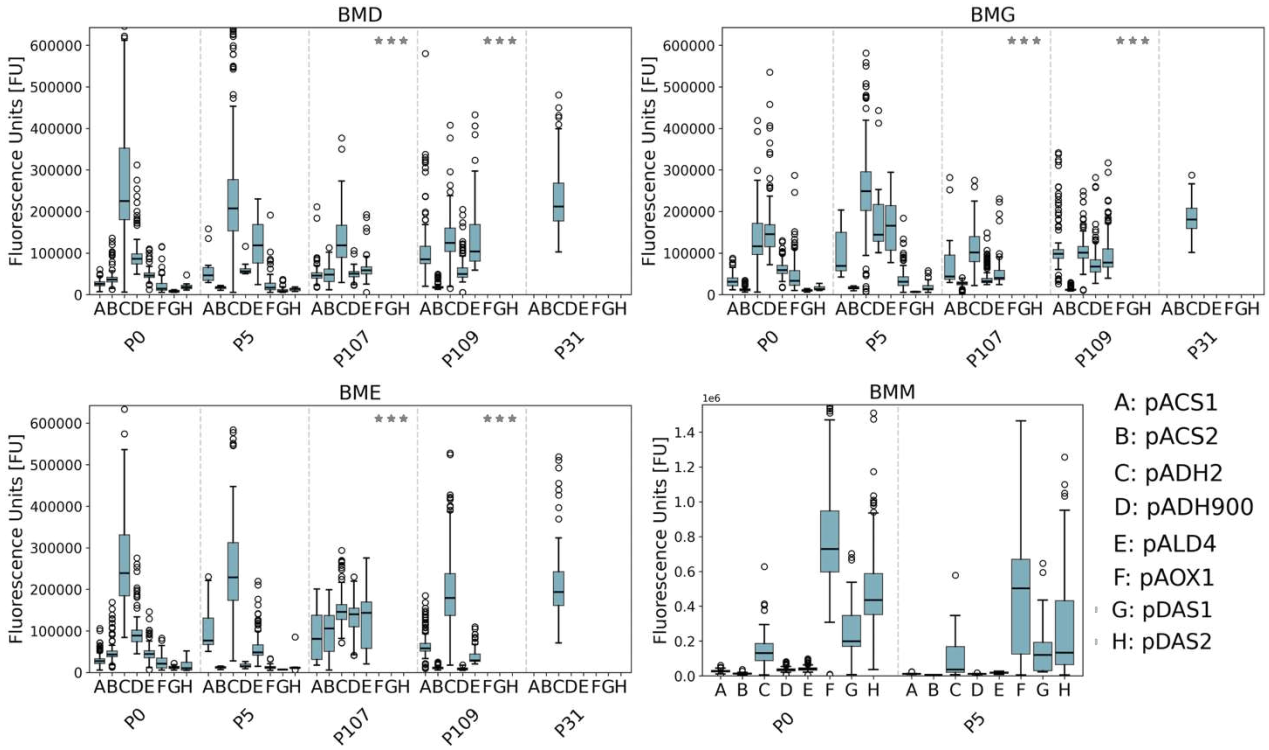


Fig. 6: eGFP levels [FU] of cultures at the end of the cultivation. Refer to figure description of Fig. 5. Star = strains not created.

Regarding P_{ADH2}, eGFP levels in P0 on BMD and BME were similar (226,00 and 239,000 FU) whereas on BMG it was half as much (128,000 FU). In P5, eGFP levels of 208,000, 250,000 and 230,000 FU were found when grown in BMD, BMG and BME, respectively. In P109 and P107, total eGFP readouts were half of those of P0 and P5 on BMD and BMG. P_{ADH2} mediated GFP expression in the *ADH2* knockout P5 was similar across all three carbon sources to P0. P_{ADH2} showed less expression on BMD and BMG in the double knockout P109 but remained relatively high on BME (180,000 FU), though still below the level of P5 (230,000 FU). Cell density-normalized eGFP levels were markedly higher in P5 and P109 compared to P0 and P107 when cultivated on BME (Fig. 7, promoter C).

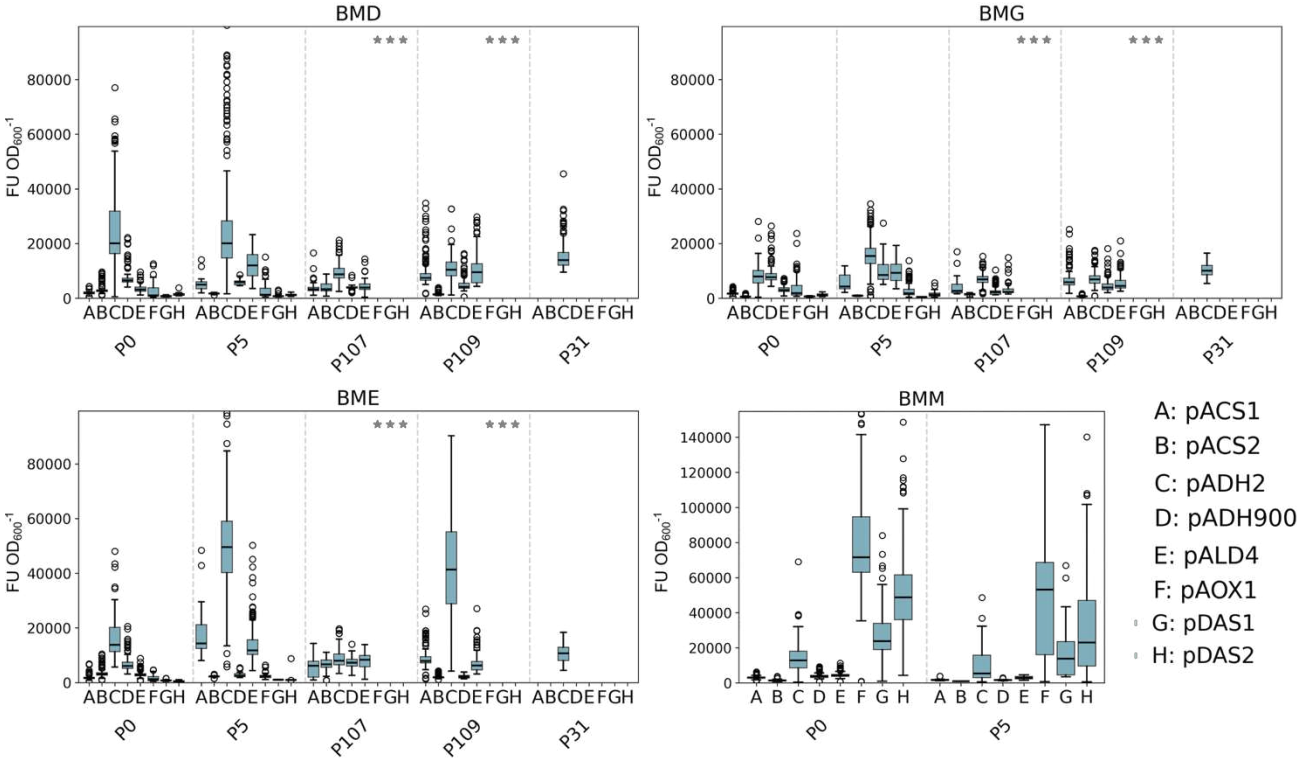
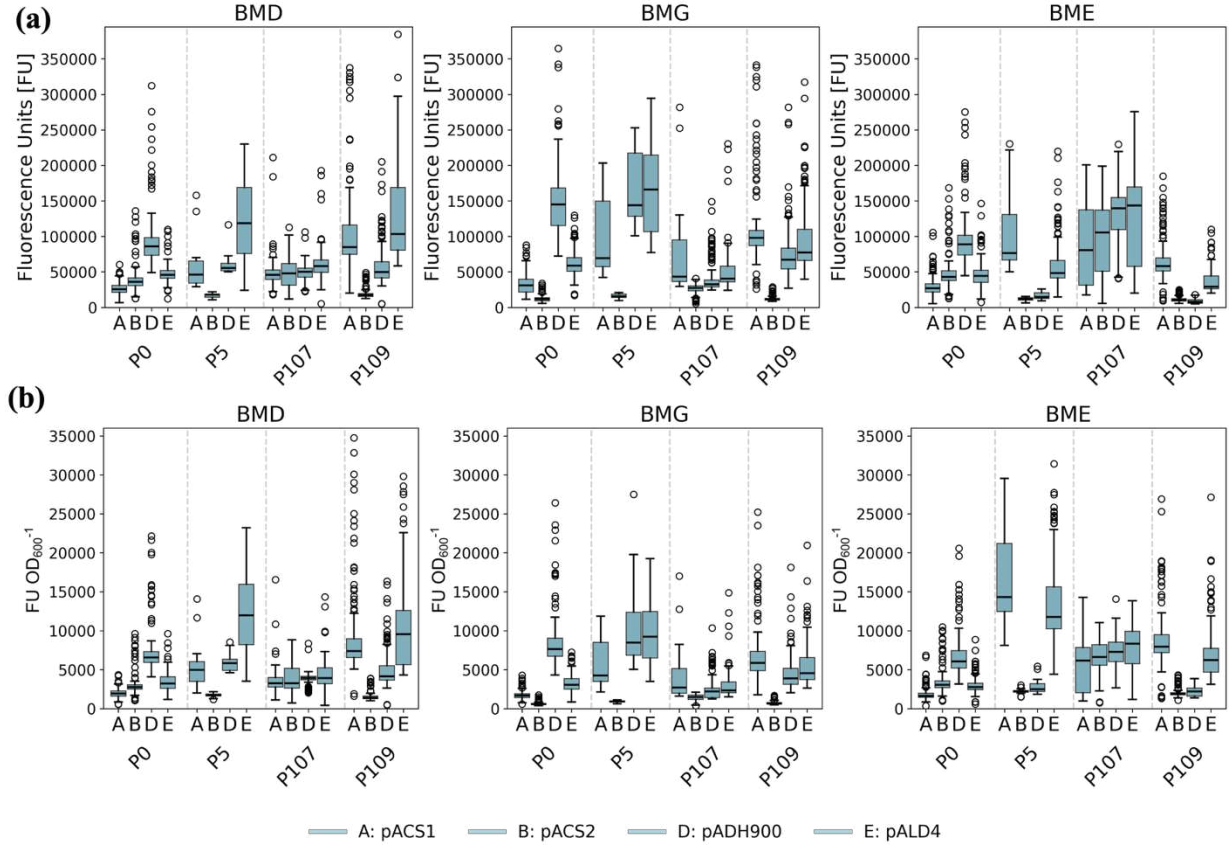


Fig. 7: eGFP levels normalized to cell density of cultures [FU OD_{600}^{-1}] at the end of the cultivation. Star = strains not created.

eGFP expression under the control of alternative EUT pathway promoters (P_{ALD4}, $P_{ACS1/2}$ and P_{ADH900}) were comparably lower than under P_{ADH2} and are therefore depicted in separate graphs for

355 better readability (Fig. 8). P107 P_{ALD4} total fluorescence on BME was 143,000 FU and 3-fold higher
356 than P0 with 45,000 FU (normalized: 8,000 FU OD_{600}^{-1} vs. 2,800 FU OD_{600}^{-1}). P5 P_{ALD4} showed
357 comparable total eGFP expression to P0 on BME, while P109 P_{ALD4} yielded the lowest total
358 readouts (29,000 FU), likely due to impaired EtOH-dependent growth, which was more severe in
359 P109 than P5. Notably, despite total expression levels, normalized eGFP values in P5 P_{ALD4} were
360 3- to 4-fold higher than in P0.



361

362 **Fig. 8:** (a) eGFP levels [FU] and (b) eGFP levels normalized to cell density of cultures [FU OD_{600}^{-1}] at the end of the
363 cultivation of strains P0, P5, P107 and P109 expressing eGFP under the control of EUT pathway promoters only.

364 P_{ACS1} values on BME were 79,000 FU and almost double to BMD (46,000 FU) and BMG (43,000
365 FU) while the differences for P_{ACS2} were even greater with 105,000 FU on BME, 48,000 FU on
366 BMD and 27,000 on BMG. Normalized eGFP levels for P_{ACS1} were threefold higher in P5 on BME
367 compared to other carbon sources, whereas for P_{ACS2} they were rather similar (Fig. 8, promoter A

and B). P_{ACS1} did not show any induction-like behavior in P0, as values were similar on BMD, BMG and BME, whereas only P_{ACS2} eGFP expression increased slightly on BME by 20%. P109 P_{ACS2} behaved similarly to P5 P_{ACS2} on BME, though normalized values were approximately 20% lower across all carbon sources. In contrast, P109 P_{ACS1} exhibited minimal total and normalized eGFP levels on BME relative to P5.

P_{ADH900} values in P0 and P107 were inverse to what we observed in P5 and P109. P0 and P107 P_{ADH900} strains showed approximately 6,000 and 7,300 FU OD_{600}^{-1} while for P5 and P109 P_{ADH900} only 2,700 and 2,500 FU OD_{600}^{-1} were measured. The highest eGFP levels found were 141,000 FU in P0 and 135,000 FU in P5 grown on BMG but strongly reduced in P107 with 32,000 FU and P109 65,000 FU. No large differences were observed for P0 and P5 vs. P107 and P109 P_{ADH900} grown in BMD.

4. Discussion

4.1 ADH2 and ADH900 show functional overlap in both directions

Three different genetically modified strains were derived from the *K. phaffii* CBS 2612 wild-type strain. First, *alcohol dehydrogenase 2* was knocked out to generate a phenotype (strain P5, Δ*ADH2*) with impaired growth on EtOH as a carbon source. This phenotype resembles the *K. phaffii* Mut^S phenotype (Δ*aox1*) which shows impaired growth on methanol. For comparison, P5 had a growth rate (μ) of 0.03 h^{-1} and a doubling time (t_d) of 20 h on EtOH while Mut^S strains typically have a μ of 0.04 h^{-1} corresponding to a doubling time of 17 h on MeOH (Higgins and Cregg, 1998; Orman *et al*., 2009). Wild-type *K. phaffii* (Mut^+) has a μ of 0.14 h^{-1} (t_d=5 h) on MeOH (Higgins and Cregg, 1998; Orman *et al*., 2009) and a μ of 0.1 h^{-1} (t_d=7 h) on EtOH (our study). Secondly, *alcohol dehydrogenase 900* was knocked out in the wild-type to generate a phenotype (P107, Δ*ADH900*), able to grow on EtOH but with impaired ability to form EtOH when grown on fermentable carbon

sources (μ=0.07 h^{-1}, t_d=10.6 h). Finally, both genes were knocked out in the wild-type to shutdown growth on EtOH completely, and fully suppress the formation of EtOH (P109, Δ*adh2* Δ*adh900*). While P5 indicated at least slow growth rates, P109 showed no growth at all on EtOH medium. Although ADH2 and ADH900 are not functionally analogous to AOX1 and AOX2, the double knockout strain (Δ*adh2* Δ*adh900*) exhibits a growth phenotype equal to the Mut^- strain lacking *AOX1* and *AOX2*, which cannot grow on MeOH (Higgins and Cregg, 1998). As highlighted by Inan *et al*., ADH900 and ADH2 primarily fulfill distinct functions - EtOH formation by reduction and EtOH consumption by oxidation, respectively. However, it was also reported that ADH2 can partially complement the function of ADH900 when absent, enabling EtOH formation from glucose (Karaoğlan *et al*., 2020). The present results suggest a functional overlap between the two enzymes. One might hypothesize that ADH900 can partially compensate for the lack of ADH2 activity, allowing for very limited growth on EtOH at a slow rate. Further support for this hypothesis comes from the finding that strain P107 displayed reduced growth rates on BME1 relative to P0.

Crab-negative yeasts like *K. phaffii* can produce certain amounts of EtOH due to glucose overflow metabolism and high cell-densities paired with oxygen limitation at later growth stages (Passoth *et al*., 2003). Up to 16 g L^{-1} of EtOH were detected when *K. phaffii* BG11 was grown in batch with 40 g L^{-1} of initial glucose concentration (4 wt %). The authors concluded that the production and accumulation of EtOH becomes minimal when grown under conditions of less than 5 g L^{-1} glucose (Steimann *et al*., 2024). Our results are in line with these reports as EtOH was present in all BMD samples (Fig. 3, top). Only with the double knockout of *ADH2* and *ADH900* the formation of EtOH could be nearly fully suppressed. A similar trend was observed by Inan *et al.* who reported the *K. phaffii* wild-type X33 to produce 1.0 g L^{-1}, Δ*ADH2* 2.1 g L^{-1}, Δ*ADH900* 0.2 g L^{-1} and Δ*adh2* Δ*adh900* 0.0 g L^{-1} EtOH (Karaoğlan *et al*., 2020). Notably, evaporation of medium and EtOH

415 during the cultivation also needs to be considered when interpreting this data (Fig 3, sterile
416 controls). It should be noticed that cells were pre-cultured in BMD1. Cellular adjustment to a new
417 carbon source was necessary when transferred to the main culture - except for main cultures in
418 BMG1. This explains the shorter lag-phase and faster consumption of glucose by strains in the
419 BMD sample group compared to the BMG and BME group, respectively.
420 Given that no substantial growth of P5 or P109 on EtOH was observed and residual EtOH could
421 be detected after the cultivation period, one can conclude that the knockout of *ADH2* and *ADH900*
422 substantially decreased the metabolization rate of EtOH.
423 With respect to the unchanged observed growth on glycerol medium, effects on the strains' glycerol
424 metabolism are rather unlikely. We could not detect any EtOH formed by the cells during the
425 cultivation on glycerol (Fig. 3). However, there have been reports on *K. phaffii* producing EtOH
426 when grown on glycerol (Chiruvolu *et al*., 1998; Uppada and Noronha, 2016). In our hands, P0
427 and P5 produced up to 0.9 and 0.4 g L^{-1} EtOH, respectively, within 24 hours under C-limiting
428 glycerol fed-batch bioreactor conditions (controlled pH of 5.5, 500 mL, data not shown). Chiruvolu
429 *et al.* hypothesized that a pH-controlled environment would favor EtOH production, as the optimal
430 pH for EtOH production in yeast is about 6.0. Still, although pH was buffered in a range of 5 to 6
431 over the cultivation period in our shake flask experiments, we could not detect EtOH in any
432 experiment with *K. phaffii* grown on glycerol.

433 *4.2 eGFP expression and growth is promoted by low EtOH feeds*

434 Before we investigated the effects of the individual knockouts on eGFP expression, we identified
435 the optimal EtOH concentration for growth and eGFP expression in 96-deep well plates to be 1%
436 (Fig. 4). EtOH concentrations ranging from 0.5 to 4% affected rather P0 than P5, reflecting its
437 intrinsically poor capacity to utilize EtOH as a sole carbon source (Fig. 4). These results indicate
438 that EtOH supplementation provides a narrow window for promoting growth. EtOH is known to

increase plasma membrane fluidity and, at higher concentrations, to compromise membrane integrity in yeasts, thereby reducing viability and impairing growth and reproduction (Ding *et al*., 2009). In addition, EtOH stress induces the expression of heat shock factors and chaperone proteins that counteract intracellular protein denaturation (Ding *et al*., 2009). In *S. cerevisiae*, exposure to 10% EtOH has been shown to repress translation and damage proteins, leading to the intracellular accumulation of insoluble aggregates (Ando *et al*., 2023; Yoshida *et al*., 2021). Consequently, cells may prioritize the refolding and degradation of damaged proteins over heterologous protein synthesis, resulting in reduced protein yields per cell. Higher EtOH concentrations than 2% in the medium did not lead to upregulated eGFP expression, due to toxic side effects. Instead, concentrations of 0.5% or 1% EtOH led to the highest expression levels in both strains while 1% EtOH led to the highest biomass (Fig. 4).

4.3 Knockout strains give valuable insight in the regulation of eGFP expression under EUT pathway promoters

A landscape of wild-type *K. phaffii* and the knock-out reporter strain clones were cultivated and fed with three different carbon sources to screen for eGFP expression and growth. While the growth behavior of the strains grown on glycerol and glucose remained similar, strain growth on EtOH was not comparable. As expected and discussed in chapter 4.2, EtOH is more toxic and growth-inhibiting to P5 and P109 than to P107 which showed similar growth behavior as P0, as ADH2 is the key enzyme for EtOH metabolization. In the case of eGFP expression under methanol-inducible promoters, we found repression of P_{AOX1} particularly in P5 and P109 strains on EtOH as the sole carbon source, likely due to EtOH accumulation (Fig. 6, Fig. 7). EtOH is known to repress the synthesis of methanol utilizing enzymes (Zhang *et al*., 2000) such as AOX1 (Inan and Meagher, 2001) and DAS1/2. This trend of repression was also evident for P_{DAS1} and P_{DAS2} according to our findings (Fig 6, promoter G&H). In contrast to MUT pathway promoters, P_{ADH2} displayed a largely

constitutive expression profile in P0 and P5 under the tested conditions (BMD, BMG, BME) rather than behaving as an inducible promoter (Fig. 6, promoter C). This profile is consistent with the transcript data of Barbay *et al.* (2021), who found no significant difference in *ADH2* transcript levels between Δ*cat8* mutants and the wild-type on glucose and glycerol, while *ADH2* transcription As shown in Fig. 3, all strains produced EtOH when grown on glucose. Therefore, it would be possible that EtOH, produced in the fermentative pathway, could induce the *ADH2* promoter. The hypothesis that EtOH produced by *K. phaffii* fermenting glucose would lead to *ADH2* transcription was also proposed by Erden-Karaoğlan (Erden-Karaoğlan *et al*., 2022). Knocking out *ADH900* decreased eGFP expression under P_{ADH2} when cells were grown on glucose or glycerol, likely due to impaired EtOH production. Further, by knocking out *ADH2* and *ADH900*, the constitutive expression pattern of P_{ADH2} could be disrupted, resulting in a more EtOH-responsive, induction-like behavior. Although we saw that increasing the amount of externally added EtOH does not result in higher expression levels (Fig. 4), we assume that a stable level of EtOH, which cannot be metabolized, might lead to enhanced transcriptional activity. The *ADH900* knockout (P107) did not show the same effect, suggesting that the consumption of EtOH counteracts the upregulation of *ADH2* transcription.

We also investigated further EUT pathway promoters P_{ALD4}, $P_{ACS1/2}$ and P_{ADH900}. Aldehyde dehydrogenases (ALD) participate in the EtOH utilization pathway by converting acetaldehyde to acetate. According to Rangarajan *et al.*, ALD6-1 is the main, non-redundant enzyme in *K. phaffii* fulfilling this function, whereas ALD4 and ALD2 seem to play a minor role (Gupta *et al*., 2021). Still, expression of eGFP under the control of P_{ALD4} in the knockout strains showed a distinct pattern (Fig. 8ab, promoter E). In contrast to P_{ADH2}, total fluorescence of P107 P_{ALD4} on BME nearly tripled compared to P0 due to the knockout of *ADH900*. We speculate that the lack of ADH900 might cause an imbalance, where the reverse conversion of acetaldehyde to EtOH is hardly possible. This

imposes pressure on the cell to upregulate ALDs for detoxification. Although we could not detect acetaldehyde in P107 in shakeflask cultivations, acetate levels of up to 14 g L^{-1} were detected in P107, in contrast to P5 and P109. Given the finding that P_{ALD4} was upregulated in P5, P107 and P109 compared to P0, we conclude that P_{ALD4} responds to EtOH but might also respond to acetate or acetaldehyde and the effect can be increased by both knockouts.

Acetyl-CoA synthetases (ACS1/2) convert acetate into acetyl-CoA. Interestingly, P_{ACS1} and P_{ACS2} were upregulated in P107 on BME compared to BMD or BMG (Fig. 8, promoter A and B). P_{ACS2} was less directly influenced by EtOH than P_{ACS1} and showed only slightly higher values in P5 (Fig. 8, promoter B). This suggests that P_{ACS2} may respond to downstream metabolites produced in P107 but not in P5, in contrast to P_{ACS1}. According to Ohsawa *et al.*, *ACS1* expression was stronger in EtOH containing medium than glucose and *vice versa* for *ACS2*, as indicated by gel electrophoresis quantification of *K. phaffii* ACS1/2-CFP (Ohsawa et al., 2018). Looking at P0 in BMD and BME, we could not find such a correlation as eGFP expression under P_{ACS1} control was similar on BMD and BME (Fig. 8, promoter A).

Finally, ADH900 is reported to be key responsible for the conversion of acetaldehyde to EtOH, and its promoter showed a distinct regulatory response. Our data suggests that *ADH900* expression may be negatively regulated by EtOH. In P5 and P109, P_{ADH900} driven eGFP expression on BME showed particularly low total and normalized eGFP readouts (Fig. 8, promoter D) compared to P0 and P107. As P5 and P109 are unable to consume EtOH, accumulated EtOH likely repressed *ADH900* promoter activity. Notably, the highest total readouts for P_{ADH900} were observed in P0 and P5 cultivated on BMG (Fig. 8, promoter D). This finding is unexpected, as yeasts typically grow respiratively on glycerol rather than performing EtOH-fermentation. Also, there was no significant difference in P_{ADH900} eGFP readouts between P0 and P5 vs. P107 and P109 when grown in BMD. Although P107 and P109 should not be able to ferment glucose to EtOH to the same extent as P0

and P5 (catalyzed by ADH900), they can redirect carbon flow, for example, to acetate. Therefore, there might be no accumulation of precursors, which potentially could upregulate *ADH900*. Still, we expected P0 and P5 P_{ADH900} samples to yield lower eGFP levels, as they should produce EtOH which could repress the P_{ADH900} promoter, as seen in BME media. We suspect that the concentration of EtOH, produced by the cell itself, might be not sufficient to observe a repressing effect on P_{ADH900} under these conditions.

5. Conclusions

In summary, the comparative analysis of the wild-type strain (P0) and the genetically modified strains P5 (Δ*ADH2*), P107 (Δ*ADH900*) and P109 (Δ*ADH2* Δ*ADH900*) revealed distinct differences in growth behavior depending on the carbon source. While all strains reached similarly high biomass on glucose and glycerol, growth on EtOH was markedly impaired in P5 and completely abolished in P109, confirming the essential role of ADH2 in EtOH assimilation. Interestingly, P5 still exhibited residual growth, suggesting partial functional compensation by ADH900, while P107 grew less efficiently than P0 on EtOH, highlighting an overlap in enzyme functionality. The HPLC data supported these findings: EtOH production was reduced in *ADH900* knockout strains and almost absent in the double knockout, while acetate accumulation was most pronounced in P0 and P107, consistent with active EtOH metabolism. No major metabolic differences were observed on glycerol, showing that ADH knockouts mainly affected EtOH-related pathways.

We further identified 1% EtOH as the optimal concentration for biomass formation, with both lower (0.5%) and higher (>2%) concentrations reducing growth and eGFP yields, the latter most likely due to EtOH toxicity. These results define the operational window where EtOH supplementation can support growth and heterologous protein expression.

Promoter activity profiling revealed that P_{ADH2} behaved largely constitutively in P0 and P5, but *ADH900* knockout disrupted this pattern and rendered expression more EtOH-responsive. Moreover, P5 and P109 showed higher cell density–normalized eGFP expression from P_{ADH2} and P_{ALD4} on EtOH, suggesting that impaired EtOH consumption can enhance transcriptional activity of EUT promoters, possibly via accumulation of acetaldehyde, acetate or EtOH. In contrast, P_{ADH900} activity was low in strains unable to metabolize EtOH, supporting the theory of repression by EtOH. *ACS1* and *ACS2* promoters showed different responses, with P_{ACS1} being more EtOH-inducible than P_{ACS2}. Taken together, these results demonstrate that EtOH metabolism in *K. phaffii* involves a complex interplay between ADH2 and ADH900, whose functions partially overlap. The elucidated regulation of EUT pathway promoters can provide a basis for future engineering strategies.

Availability of data and materials

The data that support the findings of this study are available in the supporting information.

Acknowledgements

This work was supported by the Austrian Research Promotion Agency FFG (BRIDGE Project 903607). We also thank the COMET centre acib: Next Generation Bioproduction is funded by BMK, BMDW, SFG, Standortagentur Tirol, Government of Lower Austria and Vienna Business Agency in the framework of COMET - Competence Centres for Excellent Technologies. The COMET-Funding Program is managed by the Austrian Research Promotion Agency FFG.

Ethics declaration

Author information

Supplementary Information

Additional file 1 (.docx): Supplementary information file. The file contains additional tables and graphs referenced in the manuscript.

References

Ando, R., Ishikawa, Y., Kamada, Y., Izawa, S., 2023. Contribution of the yeast bi-chaperone system in the restoration of the RNA helicase Ded1 and translational activity under severe ethanol stress. Journal of Biological Chemistry 299, 105472. https://doi.org/10.1016/j.jbc.2023.105472

Barbay, D., Mačáková, M., Sützl, L., De, S., Mattanovich, D., Gasser, B., 2021. Two homologs of the Cat8 transcription factor are involved in the regulation of ethanol utilization in *Komagataella phaffii*. Curr Genet 67, 641–661. https://doi.org/10.1007/s00294-021-01165-4

Baumann, K., Carnicer, M., Dragosits, M., Graf, A.B., Stadlmann, J., Jouhten, P., Maaheimo, H., Gasser, B., Albiol, J., Mattanovich, D., Ferrer, P., 2010. A multi-level study of recombinant *Pichia pastoris* in different oxygen conditions. BMC Syst Biol 4, 141. https://doi.org/10.1186/1752-0509-4-141

Berrios, J., Theron, C.W., Steels, S., Ponce, B., Velastegui, E., Bustos, C., Altamirano, C., Fickers, P., 2022. Role of Dissimilative Pathway of *Komagataella phaffii* (*Pichia pastoris*): Formaldehyde Toxicity and Energy Metabolism. Microorganisms 10, 1466. https://doi.org/10.3390/microorganisms10071466

Cereghino, J.L., Cregg, J.M., 1999. Heterologous protein expression in the methylotrophic yeast. FEMS Microbiology Reviews. https://doi.org/10.1111/j.1574-6976.2000.tb00532.x

Chiruvolu, V., Eskridge, K., Cregg, J., Meagher, M., 1998. Effects of Glycerol Concentration and pH on Growth of Recombinant *Pichia pastoris* Yeast 75. https://doi.org/doi.org/10.1007/BF02787771

Cregg, J.M., Tolstorukov, I.I., 2012. *P. pastoris ADH* promoter and use thereof to direct expression of proteins. Patent No. US 8,222,386 B2.

Ding, J., Huang, X., Zhang, L., Zhao, N., Yang, D., Zhang, K., 2009. Tolerance and stress response to ethanol in the yeast *Saccharomyces cerevisi*ae. Appl Microbiol Biotechnol 85, 253–263. https://doi.org/10.1007/s00253-009-2223-1

Erden-Karaoğlan, F., Karaoğlan, M., Yılmaz, G., Yılmaz, S., İnan, M., 2022. Deletion analysis of *Pichia pastoris alcohol dehydrogenase 2* (*ADH2*) promoter and development of synthetic promoters. Biotechnology Journal 17, 2100332. https://doi.org/10.1002/biot.202100332

Ergün, B.G., Gasser, B., Mattanovich, D., Çalık, P., 2019. Engineering of *alcohol dehydrogenase 2* hybrid-promoter architectures in *Pichia pastoris* to enhance recombinant protein expression on ethanol. Biotech & Bioengineering 116, 2674–2686. https://doi.org/10.1002/bit.27095

Flores, C., 2000. Carbohydrate and energy-yielding metabolism in non-conventional yeasts. FEMS Microbiology Reviews 24, 507–529. https://doi.org/10.1016/S0168-6445(00)00037-1

Gupta, A., Krishna Rao, K., Sahu, U., Rangarajan, P.N., 2021. Characterization of the transactivation and nuclear localization functions of *Pichia pastoris* zinc finger transcription factor Mxr1p. Journal of Biological Chemistry 297, 101247. https://doi.org/10.1016/j.jbc.2021.101247

Hartner, F.S., Glieder, A., 2006. Regulation of methanol utilisation pathway genes in yeasts. Microbial Cell Factories 5, 39. https://doi.org/10.1186/1475-2859-5-39

Higgins, D.R., Cregg, J.M., 1998. Pichia Protocols, 103rd ed. Humana Totowa, Totowa, New Jersey.

Inan, M., Meagher, M., 2001. The Effect of Ethanol and Acetate on Protein Expression in *Pichia pastoris*. J Biosci Bioeng. https://doi.org/10.1263/jbb.92.337

Karaoğlan, M., Erden-Karaoğlan, F., Yılmaz, S., İnan, M., 2020. Identification of major *ADH* genes in ethanol metabolism of *Pichia pastoris*. Yeast 37, 227–236. https://doi.org/10.1002/yea.3443

Karaoglan, M., Karaoglan, F.E., Inan, M., 2016. Functional analysis of alcohol dehydrogenase (*ADH*) genes in *Pichia pastoris*. Biotechnol Lett 38, 463–469. https://doi.org/10.1007/s10529-015-1993-z

Krainer, F.W., Dietzsch, C., Hajek, T., Herwig, C., Spadiut, O., Glieder, A., 2012. Recombinant protein expression in *Pichia pastoris* strains with an engineered methanol utilization pathway. Microb Cell Fact 11, 22. https://doi.org/10.1186/1475-2859-11-22

Li, P., Anumanthan, A., Gao, X.-G., Ilangovan, K., Suzara, V.V., Düzgüneş, N., Renugopalakrishnan, V., 2007. Expression of Recombinant Proteins in *Pichia pastoris*. Appl Biochem Biotechnol 142, 105–124. https://doi.org/10.1007/s12010-007-0003-x

Lin-Cereghino, J., Wong, W.W., Xiong, S., Giang, W., Luong, L.T., Vu, J., Johnson, S.D., Lin-Cereghino, G.P., 2005. Condensed Protocol for Competent Cell Preparation and Transformation of the Methylotrophic Yeast *Pichia pastoris*. BioTechniques 38, 44–48. https://doi.org/10.2144/05381BM04

Liu, Q., Li, Y., Tao, L., Yang, J., Zhang, Y., Cai, M., 2025. Rational design and characterization of enhanced alcohol-inducible synthetic promoters in *Pichia pastoris*. Appl Environ Microbiol 91, e02191-24. https://doi.org/10.1128/aem.02191-24

Liu, Y., Bai, C., Liu, Q., Xu, Q., Qian, Z., Peng, Q., Yu, J., Xu, M., Zhou, X., Zhang, Y., Cai, M., 2019. Engineered ethanol-driven biosynthetic system for improving production of acetyl-CoA derived drugs in Crabtree-negative yeast. Metabolic Engineering 54, 275–284. https://doi.org/10.1016/j.ymben.2019.05.001

Näätsaari, L., Mistlberger, B., Ruth, C., Hajek, T., Hartner, F.S., Glieder, A., 2012. Deletion of the *Pichia pastoris* KU70 Homologue Facilitates Platform Strain Generation for Gene Expression and Synthetic Biology. PLoS ONE 7, e39720. https://doi.org/10.1371/journal.pone.0039720

Nocon, J., Steiger, M.G., Pfeffer, M., Sohn, S.B., Kim, T.Y., Maurer, M., Rußmayer, H., Pflügl, S., Ask, M., Haberhauer-Troyer, C., Ortmayr, K., Hann, S., Koellensperger, G., Gasser, B., Lee, S.Y., Mattanovich, D., 2014. Model based engineering of *Pichia pastoris* central metabolism enhances recombinant protein production. Metabolic Engineering 24, 129–138. https://doi.org/10.1016/j.ymben.2014.05.011

Ohsawa, S., Nishida, S., Oku, M., Sakai, Y., Yurimoto, H., 2018. Ethanol represses the expression of methanol-inducible genes via acetyl-CoA synthesis in the yeast *Komagataella phaffii*. Sci Rep 8, 18051. https://doi.org/10.1038/s41598-018-36732-2

Orman, M.A., Çalık, P., Özdamar, T.H., 2009. The influence of carbon sources on recombinant-human- growth-hormone production by *Pichia pastoris* is dependent on phenotype: a comparison of *Mut*^{s} and *Mut*$^{+}$ strains. Biotech and App Biochem 52, 245–255. https://doi.org/10.1042/BA20080057

Passoth, V., Cohn, M., Schafer, B., Hahn-Hagerdal, B., Klinner, U., 2003. Analysis of the hypoxia-induced *ADH2* promoter of the respiratory yeast Pichia stipitis reveals a new mechanism for sensing of oxygen limitation in yeast. Yeast 20, 39–51. https://doi.org/https://doi.org/10.1002/yea.933

Prielhofer, R., Reichinger, M., Wagner, N., Claes, K., Kiziak, C., Gasser, B., Mattanovich, D., 2018. Superior protein titers in half the fermentation time: Promoter and process engineering for the glucose-regulated GTH1 promoter of *Pichia pastoris*. Biotechnology and Bioengineering. https://doi.org/doi.org/10.1002/bit.26800

Rajak, N., Dey, T., Sharma, Y., Bellad, V., Rangarajan, P.N., 2024. Unlocking Nature's Toolbox: glutamate-inducible recombinant protein production from the Komagatella phaffii PEPCK promoter. Microb Cell Fact 23, 66. https://doi.org/10.1186/s12934-024-02340-1

Steimann, T., Wegmann, J., Espinosa, M.I., Blank, L.M., Büchs, J., Mann, M., Magnus, J.B., 2024. Avoiding overflow metabolite formation in *Komagataella phaffii* fermentations to enhance recombinant protein production. J Biol Eng 18, 54. https://doi.org/10.1186/s13036-024-00453-0

Uppada, V., Noronha, S., 2016. Functional characterization of alcohol dehydrogenase from Crabtree-negative yeast Komagataella (Pichia) pastoris. Current Science 111, 1596–1598. https://doi.org/https://www.jstor.org/stable/24909397

Van Der Klei, I.J., Yurimoto, H., Sakai, Y., Veenhuis, M., 2006. The significance of peroxisomes in methanol metabolism in methylotrophic yeast. Biochimica et Biophysica Acta (BBA) - Molecular Cell Research 1763, 1453–1462. https://doi.org/10.1016/j.bbamcr.2006.07.016

Van Peteghem, L., Sakarika, M., Matassa, S., Rabaey, K., 2022. The Role of Microorganisms and Carbon-to-Nitrogen Ratios for Microbial Protein Production from Bioethanol. Appl Environ Microbiol 88, e01188-22. https://doi.org/10.1128/aem.01188-22

Wang, X., Zhang, X., Mao, Y., Wu, Y., Lv, X., Liu, L., Han, W., Yin, S., Wu, R., Chen, J., Liu, Y., 2025. Ethanol-Inducible Bioproduction of Human α-Lactalbumin in *Komagataella phaffii*. J. Agric. Food Chem. 73, 9246–9260. https://doi.org/10.1021/acs.jafc.5c01338

Yoshida, M., Kato, S., Fukuda, S., Izawa, S., 2021. Acquired Resistance to Severe Ethanol Stress in Saccharomyces cerevisiae Protein Quality Control. Appl Environ Microbiol 87, e02353-20. https://doi.org/10.1128/AEM.02353-20

Zhang, W., Inan, M., Meagher, M.M., 2000. Fermentation strategies for recombinant protein expression in the methylotrophic yeast *Pichia pastoris*. Biotechnol. Bioprocess Eng. 5, 275–287. https://doi.org/10.1007/BF02942184

Supplementary Files

This is a list of supplementary files associated with this preprint. Click to download.

- SIGojWinklerMicrobCellFactsubmission.docx